



HAL
open science

Palladium-Catalyzed C-H Functionalization and Flame-Retardant Properties of Isophosphinolines

Karen-Pacelye Mengue Me Ndong, Mina Hariri, Gabin Mwande-Maguene, Jacques Lebibi, Fatemeh Darvish, Christine Safi, Kouceila Abdelli, Adam Daïch, Claire Negrell, Rodolphe Sonnier, et al.

► **To cite this version:**

Karen-Pacelye Mengue Me Ndong, Mina Hariri, Gabin Mwande-Maguene, Jacques Lebibi, Fatemeh Darvish, et al.. Palladium-Catalyzed C-H Functionalization and Flame-Retardant Properties of Isophosphinolines. *Molecules*, 2024, 29 (21), pp.5104. 10.3390/molecules29215104 . hal-04769736

HAL Id: hal-04769736

<https://imt-mines-ales.hal.science/hal-04769736v1>

Submitted on 6 Nov 2024

HAL is a multi-disciplinary open access archive for the deposit and dissemination of scientific research documents, whether they are published or not. The documents may come from teaching and research institutions in France or abroad, or from public or private research centers.






L'archive ouverte pluridisciplinaire **HAL**, est destinée au dépôt et à la diffusion de documents scientifiques de niveau recherche, publiés ou non, émanant des établissements d'enseignement et de recherche français ou étrangers, des laboratoires publics ou privés.



Distributed under a Creative Commons Attribution 4.0 International License

Article

Palladium-Catalyzed C-H Functionalization and Flame-Retardant Properties of Isophosphinolines

Karen-Pacelye Mengue Me Ndong ^{1,2} , Mina Hariri ^{1,3}, Gabin Mwande-Maguene ² , Jacques Lebibi ², Fatemeh Darvish ³, Christine Safi ⁴, Kouceila Abdelli ⁴ , Adam Daïch ⁴ , Claire Negrell ¹, Rodolphe Sonnier ⁵ , Loïc Dumazert ⁵, Abdou Rachid Issaka Ibrahim ⁶, Ilagouma Amadou Tidjani ⁶, David Virieux ¹, Tahar Ayad ^{1,*} and Jean-Luc Pirat ^{1,*}

- ¹ ICGM, Univ Montpellier, ENSCM, CNRS, 34090 Montpellier, France; guemenkaren@gmail.com (K.-P.M.M.N.); mina.hariri67@yahoo.com (M.H.); claire.negrell@enscm.fr (C.N.); david.virieux@enscm.fr (D.V.)
- ² Université des Sciences et Techniques de Masuku, Franceville BP 942, Gabon; gabin.maguene@gmail.com (G.M.-M.); jlebibi@hotmail.com (J.L.)
- ³ Department of Chemistry, K. N. Toosi University of Technology, Tehran 19991-43344, Iran; darvish@kntu.ac.ir
- ⁴ Université Le Havre Normandie, Normandie Univ, URCOM UR 3221, FR CNRS 3038, 76600 Le Havre, France; christine.safi@univ-lehavre.fr (C.S.); kouceila.abdelli@etu.univ-lehavre.fr (K.A.); adam.daich@univ-lehavre.fr (A.D.)
- ⁵ Polymers Composites and Hybrids (PCH), IMT Mines Ales, 30319 Ales, France; rodolphe.sonnier@mines-ales.fr (R.S.); loic.dumazert@mines-ales.fr (L.D.)
- ⁶ University Abdou Moumouni of Niamey, Niamey BP 10896, Niger; abdrachid2i@gmail.com (A.R.I.I.); ilagoumat@gmail.com (I.A.T.)
- * Correspondence: tahar.ayad@enscm.fr (T.A.); jean-luc.pirat@enscm.fr (J.-L.P.); Tel.: +33-448-792-015 (T.A.); +33-448-792-014 (J.-L.P.)

Abstract: C-H activation is a powerful strategy for forming C-C bonds without the need for pre-functionalization. In this paper, we present a general, direct, and regioselective palladium-catalyzed functionalization of a phosphorus heterocycle, 2-phenyl-1*H*-isophosphinoline 2-oxide. The mild reaction conditions enabled the introduction of various functionalized alkenes. Moreover, the flame-retardant properties of selected products clearly highlighted the synergy between the phosphine oxide and another heteroatom-based group, even in the condensed phase.

Keywords: C-H functionalization; isophosphinoline oxide; flame retardant; regioselective palladium-catalyzed



Citation: Mengue Me Ndong, K.-P.; Hariri, M.; Mwande-Maguene, G.; Lebibi, J.; Darvish, F.; Safi, C.; Abdelli, K.; Daïch, A.; Negrell, C.; Sonnier, R.; et al. Palladium-Catalyzed C-H Functionalization and Flame-Retardant Properties of Isophosphinolines. *Molecules* **2024**, *29*, 5104. <https://doi.org/10.3390/molecules29215104>

Academic Editor: Gianfranco Favi

Received: 27 September 2024

Revised: 18 October 2024

Accepted: 24 October 2024

Published: 29 October 2024



Copyright: © 2024 by the authors. Licensee MDPI, Basel, Switzerland. This article is an open access article distributed under the terms and conditions of the Creative Commons Attribution (CC BY) license (<https://creativecommons.org/licenses/by/4.0/>).

1. Introduction

Cross-coupling reactions, discovered over 50 years ago, have evolved into a mature technology with significant impact and impressive advancements both in academia and industry [1]. Current research focuses on enhancing the efficiency of these reactions and broadening their scope, with the understanding that even minor improvements in catalyst efficiency can lead to substantial economic benefits [2–4]. Typically, C–C bond formation via cross-coupling reactions involves a transition metal-catalyzed reaction between a halogenated derivative and an organometallic species. However, the need for multiple synthetic steps to prepare the halogenated derivative and/or organometallic reagents represents one of the few limitations of these otherwise robust synthetic tools. In contrast, transition-metal-catalyzed C–H activation has recently emerged as an efficient and streamlined alternative to traditional coupling reactions [5]. By directly functionalizing the C–H bond, these new strategies circumvent the need for cumbersome pre-functionalization steps, thereby offering greater atom economy, reduced waste, and time efficiency [6–8]. Notably, recent advances in direct C(sp²) C–H functionalization have facilitated the modification of *N*- and *O*-heterocycles [9].

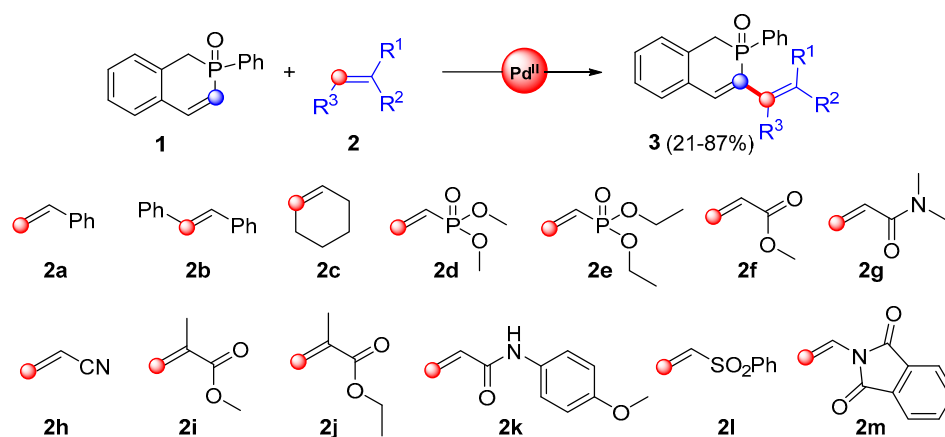
Otherwise, in the field of heteroatom chemistry, organophosphorus compounds constitute a diverse class of molecules that have attracted the attention of synthetic chemists and industry alike. They are versatile molecules with plentiful applications across domains as diverse as organic synthesis [10,11], including agrochemicals [12], pharmaceuticals [13,14], and cosmetics [15]. Moreover, they have found drawn interest in the field of material science as building blocks to elaborate functional polymers [16], metal organic frameworks (MOFs) [17,18], and electroluminescent materials [19]. Even when organophosphorus compounds are not the primary constituent of a material, they contribute significantly. For instance, they can act as photo-initiators [20] or impart key properties, enabling the recovery of strategic metals [21], or functioning as flame retardants [22–25].

Despite their importance, the design of novel phosphorus-based molecules remains highly desirable. Phosphorus heterocycles, where phosphorus atoms are embedded within the heterocyclic core have received less attention, aside from DOPO, which is one of the most recent commercial successes in the flame-retardant industry. Furthermore, the post-functionalization of such building blocks remains an under-explored area. Within the scope of our ongoing project dedicated to the development of isophosphinoline building blocks, recently reported by our group [26], we describe herein their regioselective direct C-2 functionalization through atom-economic C–H activation reactions. We envision achieving this task through reactions with different Michael acceptors. To the best of our knowledge, there are no reported examples of direct regioselective C-2 functionalization reactions of vinylphosphine oxide derivatives or phosphorus-containing heterocycles, including isophosphinolines. In 2021, Zhang first reported the synthesis of P-stereogenic phosphinates through allylic alkylation of *H*-phosphinates [27]. To illustrate the potential of these new molecules, alongside the development of a novel C–H coupling reaction, we will explore their applications as flame retardants.

2. Results and Discussion

2.1. C-H Functionalization of Isophosphinolines Catalyzed with Palladium Acetate

For the preliminary study, we employed 2-phenyl-1*H*-isophosphinoline 2-oxide (**1**) as model substrate. This compound had been previously synthesized by our group [26]. Under the conditions described by one of us [6], we engaged isophosphinoline 2-oxide (**1**) with various terminal, internal, and functionalized alkenes in the presence of palladium acetate (10 mol%) as a catalyst, silver carbonate (1.17 eq.) as an oxidant, and pivalic acid (4 mL) as an additive (Scheme 1). The reactions were heated at 90 °C for 20 h. Based on the results presented in Table 1, it is clear that the effectiveness of the C–H functionalization is strongly influenced by the nature of the vinyl partners.



Scheme 1. C–H functionalization of 1*H*-isophosphinoline 2-oxide (**1**) catalyzed with Pd(OAc)₂.

Table 1. Regioselective C2 functionalization of 1*H*-isophosphinoline 2-oxide (1) with alkenes.

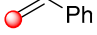
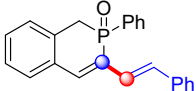
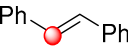
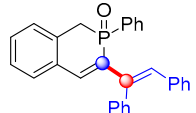
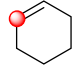
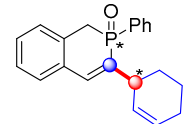
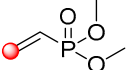
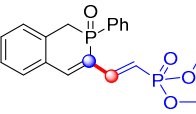
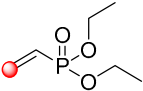
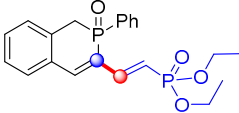
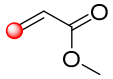
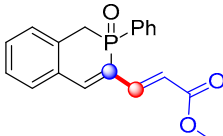
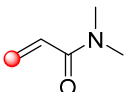
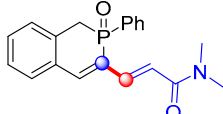
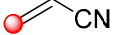
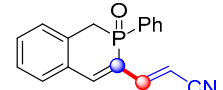
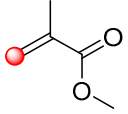
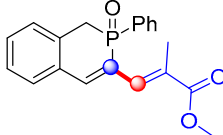
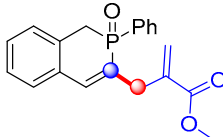
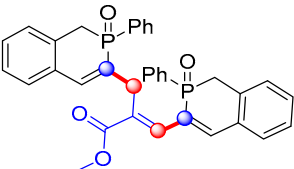
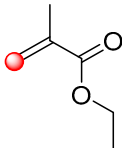
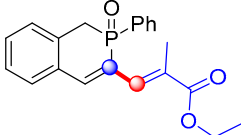
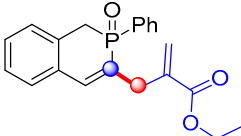
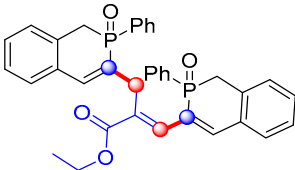
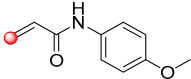
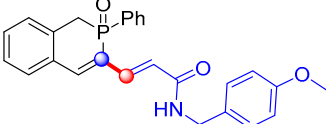
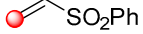
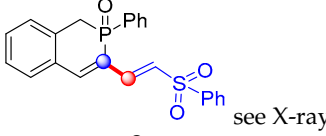
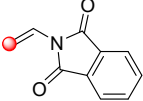
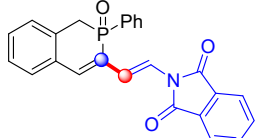
Entry	Alkene 2	Alkene 2 (Structure)	Product 3	Product 3 ¹ (Structure)	Yield ² (in %)
1	2a		3a		57
2	2b		3b		28
3	2c		3c		38
4	2d		3d		50
5	2e		3e		87
6	2f		3f		59
7	2g		3g		25
8	2h		3h		44
9	2i		3ia		4
			3ib		10
			3ic		25

Table 1. Cont.

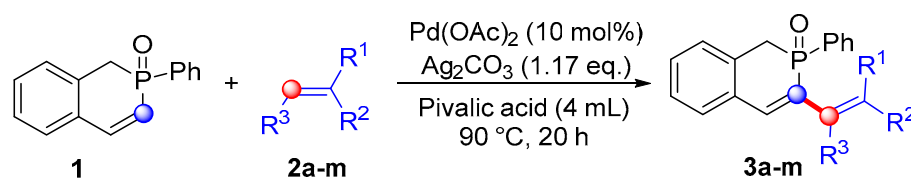
Entry	Alkene 2	Alkene 2 (Structure)	Product 3	Product 3 ¹ (Structure)	Yield ² (in %)	
10	2j		3ja		4	
				3jb		31
				3jc		27
11	2k		3k		31	
12	2l		3l	 see X-ray	37	
13	2m		3m		21	

¹ Only the C2-functionalized isomer was produced. ² Yields are reported after isolation and purification by silica gel flash column chromatography.

2.2. C-H Functionalization Discussion

When alkenes such as styrene (Table 1, entry 1, **2a**) or trans-stilbene (Table 1, entry 2, **2b**) were used, the corresponding coupling products **3a** and **3b** were isolated after treatment and purification by column chromatography, with yields of 57% and 28%, respectively. Surprisingly, the reaction of cyclohexene (Table 1, entry 3, **2c**) resulted in the formation of a regioisomer **3c** of the expected product in 38% isolated yield. Such isomerization is not so rare and typically occurs during the reductive β -elimination step [28–30]. Alkenes bearing electron-withdrawing groups, such as methyl or ethyl vinylphosphonates, (**2d**) and (**2e**), and methyl acrylate (**2f**), afforded the corresponding adducts in yields ranging from 50% up to 87%. The reactions were totally regioselective, as only coupling at the C2 position of the isophosphinoline 2-oxide (**1**) was observed. For these unsymmetrical alkenes, the reactions also occurred regio- and stereoselectively, forming (*E*)-isomers (Table 1, entries 4–6). Similarly, *N,N*-dimethylacrylamide (**2g**) and acrylonitrile (**2h**) furnished the corresponding products **3g** and **3h** in isolated yields of 25% and 44%, respectively (Table 1, entries 7 and 8). The same regio- and stereoselectivity was observed, as described by Hong group [26]. From these reactions, it becomes evident that the phosphoryl group (P=O) acts as an effective “ortho-directing group”, thereby promoting the reaction exclusively at the C2 position. In contrast, when methyl methacrylate (**2i**) and ethyl methacrylate (**2j**) were used as reagents, a mixture of two regioisomers **3ia-b** and **3ja-b**, along with compounds **3ic** and **3jc** resulting from double activation, were formed (Table 1, entries 9 and 10). Following isolation

through column chromatography, the structures of these compounds were assigned using proton NMR analysis. They are consistent with the observations reported by Hong in the studies involving the regioselective palladium-catalyzed olefination of coumarins via aerobic oxidative Heck reactions [31]. Of interest, isophosphinolines **3ib** and **3jb** were alkene-regioisomers of **3ia** and **3ja**, respectively, as previously observed for product **3c**. The double adducts **3ic** and **3jc** resulted, for their part, from a double C–H activation. They were directly formed from **3ib** and **3jb** by reaction with isophosphinoline (**1**). Primary amides, such as *N*-(4-methoxybenzyl)acrylamide (**2k**) or phenylvinylsulfone (**2l**) also afforded the corresponding adducts **3k** and **3l**, respectively, without reaction alteration with NH amide in the case of **3k**. Finally, an electron-rich alkene, 2-vinylisoindoline-1,3-dione (**2m**), was engaged successfully in this reaction, furnishing a single isomer **3m**, albeit in low yield. The structure of **3** was also confirmed by X-ray analysis of one representative example, compound **3l** (see Scheme 2, Figure 3 and ESI).



Scheme 2. Regioselective C2 functionalization of 2-phenyl-1*H*-isophosphinoline 2-oxide (**1**).

3. Flame-Retardant Potential of Certain Molecules

Despite the moderate yields obtained in certain cases, we decided to investigate the potential flame-retardant properties of some of our new phosphorus-containing heterocycles.

Flammability of Functional Isophosphinolines Results and Discussion

To assess the flame-retardant effect of one molecule, it is essential to test it within a polymer matrix. However, assessing the thermal decomposition of the molecule alone can provide useful information if it undergoes pyrolysis rather than vaporization, which is effectively the case for isophosphinolines due to their high molecular mass and the poor volatility associated with phosphoryl-based molecules.

Thermogravimetric analyses under nitrogen flow (anaerobic pyrolysis) and a microscale combustion calorimeter were carried out to assess the pyrolysis and flammability behavior of several isophosphinolines. The data are listed in Tables 2 and 3, and some thermogravimetric (TG) and heat release rate (HRR) curves are shown in Figures 1 and 2, respectively.

Based on these analyses, three distinct groups of isophosphinolines can be considered. The first group includes compounds **3a** and **3b**, which are molecules with only aromatic substituents. These isophosphinoline derivatives exhibit very low residue at 750 °C in thermogravimetric analysis (TGA) and microscale combustion calorimetry (MCC) around 5 wt%, although their residues are slightly superior compared to triphenylphosphine oxide (TPPO), which was used as a phosphine oxide reference. Consequently, the total heat release was high (23.8 kJ.g^{−1} for **3b**). This observation aligns with previous findings [30] about the contributions of different groups to fire properties. Aromatic groups have effective flame-retardant properties only when they contain a heteroatom or are linked to specific oxygen, nitrogen, or sulfur-bearing groups (such as esters, ketones, amides, or sulfonyls). A phenyl group alone significantly contributes to heat release (35 kJ.g^{−1}) and heat release capacity (900 J.g^{−1}.K). This explains why the pHRR of compound **3b** was also relatively high (230 W.g^{−1}), while its rate of degradation in TGA was higher than for **3a**.

These molecules, **3a** and **3b**, decomposed into one main peak centered at 334–338 °C in TGA and 400 °C in MCC. The heating rate was higher in MCC than in TGA; therefore, peak temperatures were usually delayed. For comparison, the thermal decomposition of TPPO also occurred in a single step with a maximum temperature of 358 °C, close to the temperatures observed for **3a** and **3b**, which were higher than the decomposition temperatures of more oxidized phosphorus-containing analogues (phosphates or phosphonates).

The temperature for 5 wt% of mass loss was around 150 °C, and was slightly higher for **3b**, probably due to a higher molecular weight and steric hindrance.

Most articles indicate that phosphine oxides are poor char promoters and have high activity in the gas phase, which is confirmed here. The flame inhibition effect cannot be observed in TGA (where only pyrolysis is measured), nor in MCC (where combustion is forced to be complete). Char promotion may be enhanced by adding functional groups to contribute to a dual mode of action (combining effects in both condensed and gas phases). Increasing residues can limit the formation of combustible gas, and the barrier effect due to a char layer is more expected when the char content is high.

Table 2. TGA values of some interesting functionalized isophosphinolines.

Sample	Td5% (°C)	Td Max (°C)	pMLR ¹ (%/°C)	Residue at 750 °C (in %)
3a	140	≈210 ²	0.1821	6.6
		338	0.5131	
3b	165	334	1.221	4.1
3d	169	324	0.1985	32.5
		411	0.5572	
		450	0.3703	
3e	106	292	0.3403	27.7
		405	0.3719	
3f	211	310	0.2780	21.8
		449	0.5421	
3g	245	358	0.5269	20.6
		423	0.4662	
3h	162	327	0.4218	13.8
		421	0.5884	
3ib	161	293	0.5035	22.7
		437	0.1481	
3ja	160	178	0.1236	23.1
		300	0.5313	
		428	0.1237	

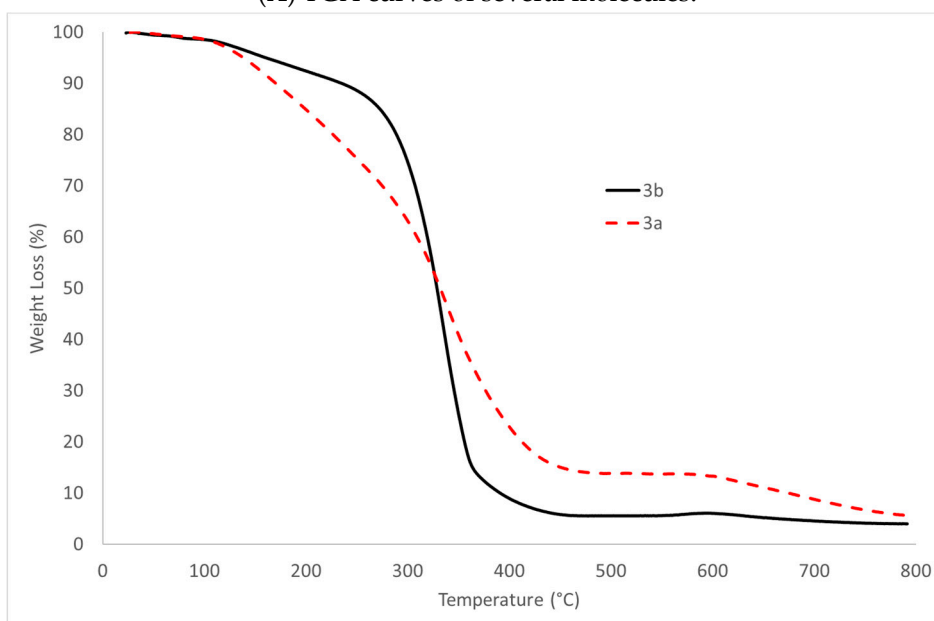
¹ pMLR: peak of mass loss rate. ² Shoulder.

Table 3. Main data measured in PCFC for several molecules.

Sample	pHRR1 (W.g ⁻¹)	TpHRR1 (°C)	pHRR2 (W.g ⁻¹)	TpHRR2 (°C)	THR (kJ.g ⁻¹)	Residue (wt%)	ΔH (kJ.g ⁻¹)
3b	230	400	-	-	23.8	3.9	24.8
3d	51	353	178	445	16.2	32.4	24.0
3e	175	329	98	413	19.1	32.5	28.3
3f	59	351	188	472	20.7	25.7	27.9
3g	150	395	195	462	22	20.4	27.6
3h	128	381	177	452	22.5	20.4	28.3
3ja	118	317	40	463	14.5 ¹	24	19.1 ¹

¹ Doubtful data, due to early decomposition.

(A) TGA curves of several molecules.



(B) Ester or amide or nitrile-containing isophosphinolines.

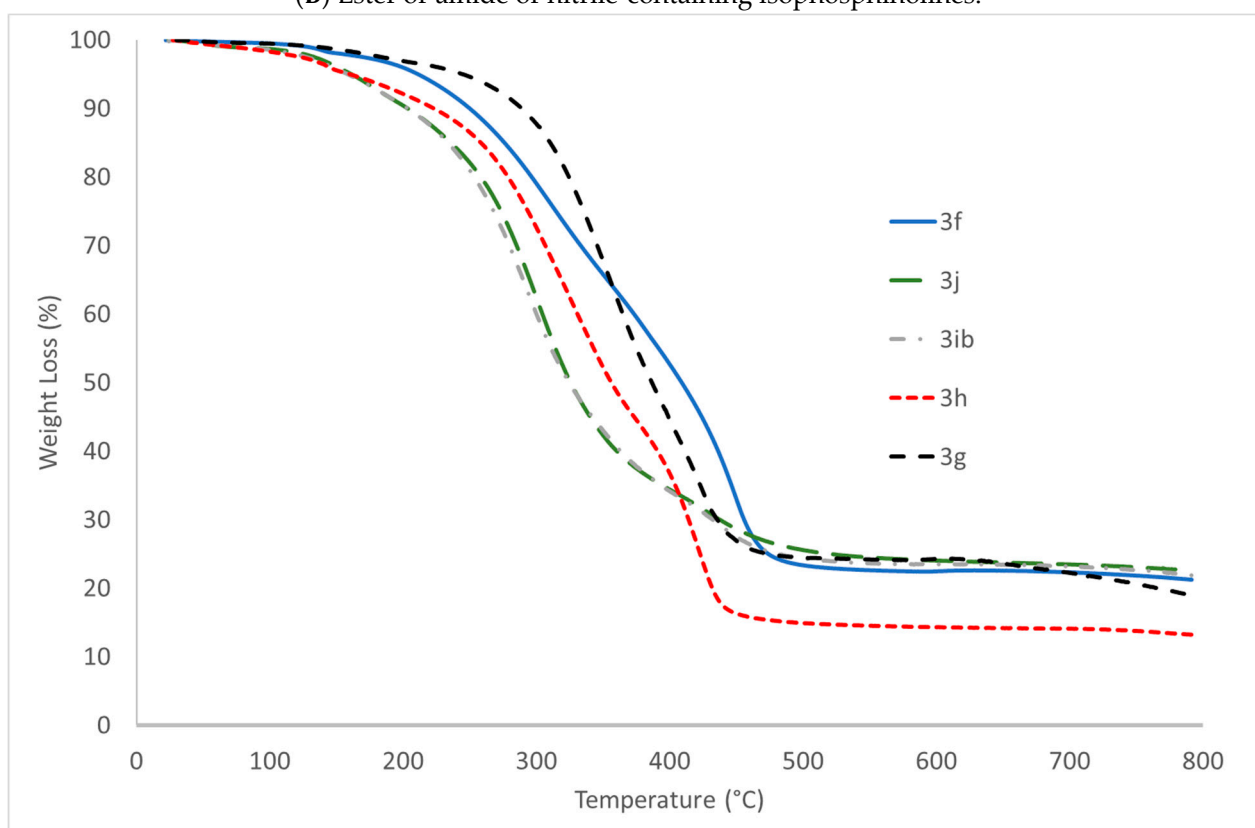


Figure 1. Cont.

(C) Phosphonate-containing isophosphinolines.

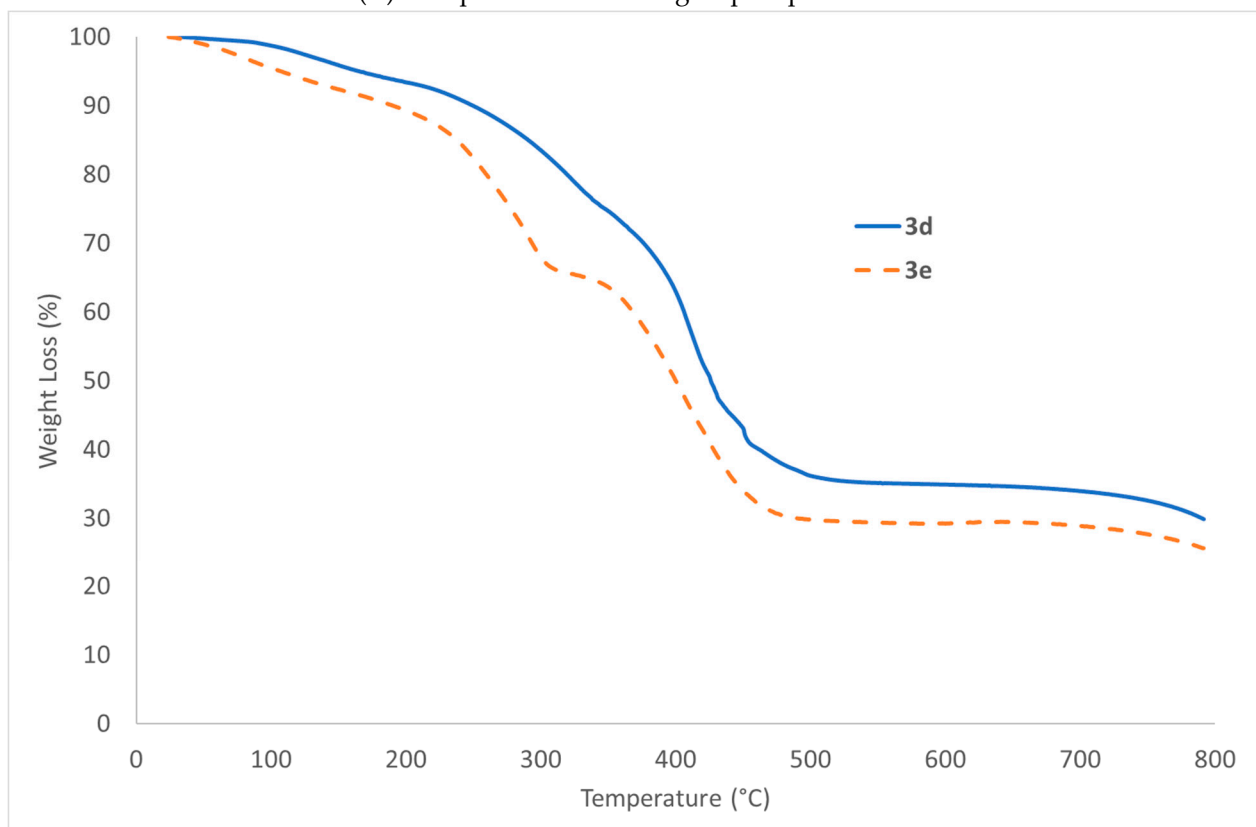


Figure 1. TGA curves of several molecules **3**: (A) Phenyl-containing isophosphinolines, (B) ester or amide or nitrile-containing isophosphinolines, and (C) phosphonate-containing isophosphinolines.

For all molecules tested, except for **3a** and **3b**, the decomposition was more complex with at least two peaks, and the residue content was much higher. Molecules containing substituents such as nitrile, ester, or amide groups exhibited residue contents higher than 20 wt% (except for **3h**–13.8 wt%) in TGA. The residue content in MCC was also significantly improved (20.4 wt% for **3g** and **3ja**).

The Td5% of these molecules was higher, ranging from 160 °C to 245 °C for **3g**. The first main peak of decomposition in TGA was usually close to 300 °C, which was lower than the decomposition peak of **3a** and **3b**. However, the second peak occurred at a much higher temperature than the main decomposition peak of TPPO (at 400 °C). This temperature was increased by a few dozen degrees for other molecules with functional groups carrying heteroatoms.

In MCC, the HRR curves also exhibited two peaks for these nitrogen-containing molecules. The first peak occurred near 400 °C for **3h** and **3g** ($\text{pHRR} = 128\text{--}150 \text{ W}\cdot\text{g}^{-1}$), and a higher second peak ($177\text{--}195 \text{ W}\cdot\text{g}^{-1}$) was observed at a high temperature (452–462 °C). These two peaks were also visible in TGA curves, but were slightly lower compared to those observed in MCC ones. Molecules **3f** and **3ja**, which contained an ester group, exhibited lower thermal stability, with a first peak in the range of 300–350 °C. The residue contents were similar to those obtained in TGA (20 wt%). The THR remained high ($22\text{--}22.5 \text{ kJ}\cdot\text{g}^{-1}$), and the heat of complete combustion reached around 28 kJ/g, except for molecule **3ja**, which exhibited the lowest THR. However, its decomposition started at a very low temperature (before 150 °C), which may explain why the heat release was not fully recorded in MCC. For the two first groups, an acceleration of degradation was observed from 300 °C, with a pMLR greater than $\approx 0.4\%/^{\circ}\text{C}$ (based on TGA data).

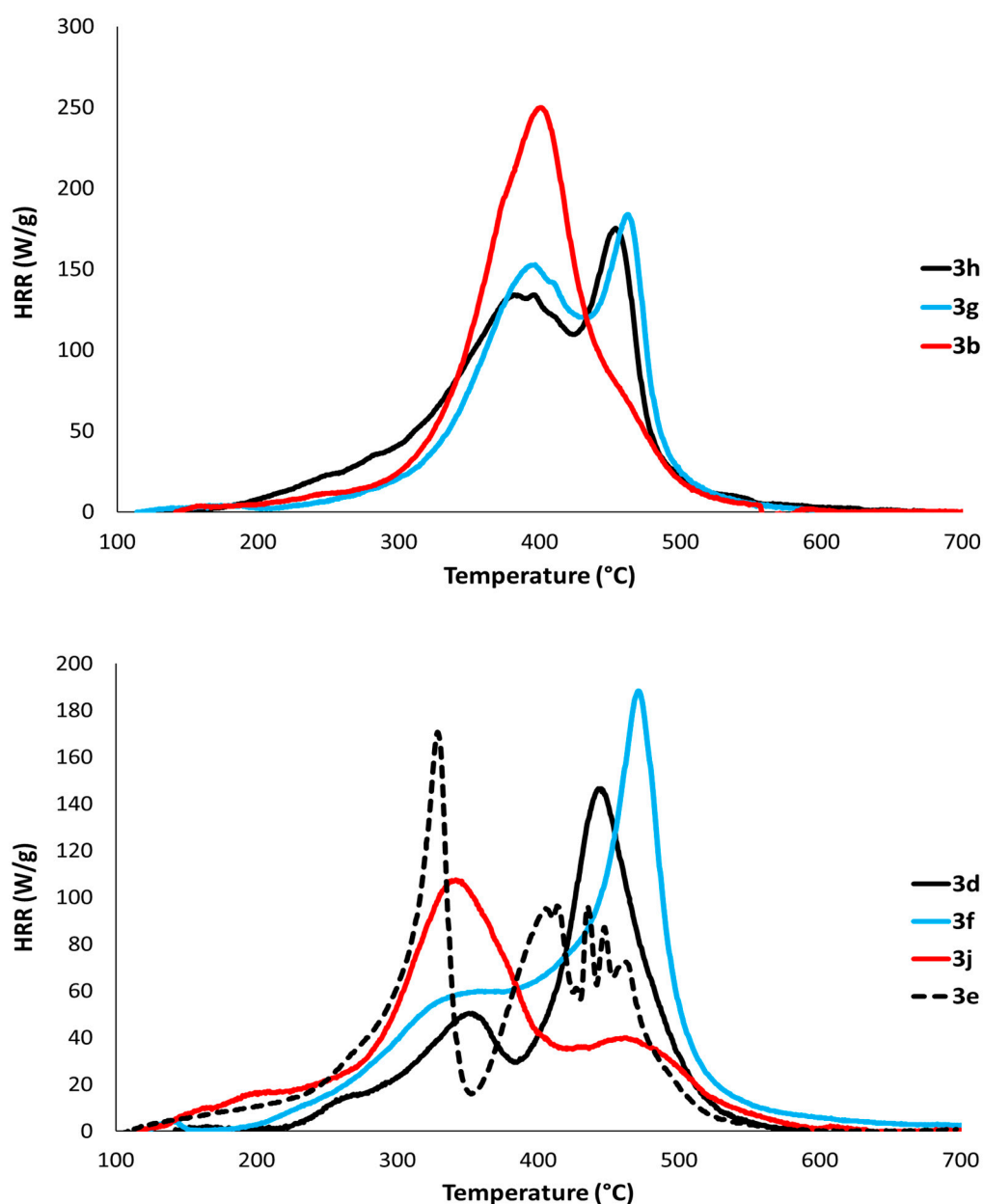


Figure 2. HRR curves of several molecules measured in MCC.

The third group consisted of molecules **3d** and **3e**, which contained a phosphonate group. Both molecules exhibited the highest residue content in both TGA and MCC (around 30 wt%), confirming that phosphonate groups, with a higher degree of oxidation of the phosphorus atom, enhance charring. Thus, examining products **3e** and **3d**, our team has already observed and confirmed the difference in degradation temperature $T_{d5\%}$ between the two phosphonate-containing isophosphinolines [31]. Indeed, the methoxy group is more stable than the ethoxy group. This aligns with the lowest THR observed for both molecules (excluding **3ja**, as previously discussed). Both molecules also exhibited a two-step decomposition, but their thermal stability was relatively lower compared to other isophosphinolines, which is typical for molecules containing phosphate or phosphonate groups. Indeed, in MCC, the first peak was observed in the range 300–350 °C, while the second peak appeared above 400 °C. Moreover, compound **3e**, which had ethyl phosphonate groups, showed premature decomposition with a $T_{d5\%}$ close to 100 °C. In MCC, the HRR increased from the beginning of the test, similar to **3ja**.

An interesting observation was made concerning residue. Phosphonate-based isophosphinolines were the only molecules leaving expanded residue at the end of the MCC test. These molecules should be able to promote intumescence, a mode of action very effective in flame retardancy: the formation of a porous, expanded, and thermally stable char layer allows drastic limitations to the heat diffusion from the flame to the underlying material.

Note that the first peak was higher for **3e** compared to **3d**, and for **3ja** compared to **3f**. This tendency was reversed for the second peak, which was higher for **3d** and **3f**. This difference can be ascribed to the presence of ethoxy groups in **3e** and **3ja**, as opposed to the methyl groups found in **3d** and **3f**. These groups likely do not participate in char formation and are probably eliminated at lower temperatures. According to our previous work, the contributions to HRC (heat release capacity, which is equal to the pHRR divided by the heating rate) were 1200 and 1400 J.g⁻¹.K for the methylene (CH₂) and methyl (CH₃) groups, respectively. Therefore, considering that these groups were involved in the first decomposition peak, the first peak in both TGA and MCC was higher for compounds **3e** and **3j**. Moreover, ethyl groups are generally much less thermally stable than methyl groups, as evidenced by the much lower thermal stability of molecules **3e** and **3ja**.

Some conclusive remarks can be drawn from these results. Isophosphinoline heterocycles are not able to engage in self-charring, despite their highly aromatic structure. However, the presence of functional groups such as esters, amides, nitriles, and especially phosphonates as substituents of the phospho-heterocycle significantly enhances charring. Seibold's group, when studying the 2,8-dimethyl-phenoxy-phosphin-10-oxide (DPPO) thermal decomposition, have already highlighted the high residue content for phosphine oxides with oxygen synergy [32]. The association of a phosphine oxide with another heteroatom-carrying group induces a synergy that enables action in the condensed phase. This phenomenon is not typically observed in pure phosphine oxide-based *flame-retardants* (FRs). This property makes these molecules promising candidates for future use as FRs in polymers such as epoxies, polyesters, etc. However, this synergy often leads to a more complex decomposition pathway, involving multiple steps at low temperatures. Specifically, the presence of ethyl groups on esters or phosphonates seems to be detrimental to thermal stability. This difference can be attributed to a facilitated internal elimination mechanism (Ei) [27]. Syn-elimination, a thermal process often observed during pyrolysis, occurs through a cyclic 6-membered ring transition state, which is only possible for ethyl-substituted phosphonates.

4. X-Ray Crystallography

Single-crystal X-ray diffraction data were collected on a Rigaku XtaLAB Synergy-S, Dualflex diffractometer equipped with a HyPix-6000HE Hybrid Photon Counting (HPC) detector. The unit cell determination and data integration were carried out using the CrysAlisPro package (Version CrysAlisPro 1.171.39.29c, Rigaku OD, 2017) from Oxford Diffraction [33]. Multi-scan correction for absorption was applied. The structures were solved with the SHELXT 2018/2 structure solution program using the Intrinsic Phasing method and refined by the full-matrix least-squares method on F² with SHELXL 2018/3 [34,35]. Olex2 was used as an interface to the SHELX programs [36]. Non-hydrogen atoms were refined anisotropically. Hydrogen atoms were added in idealized positions and refined using a riding model. Crystal data, data collection, and structure refinement details are provided in the electronic supporting information and the corresponding CIF files. CCDC-2386195 contains the supplementary crystallographic data for this paper. These data can be obtained free of charge from The Cambridge Crystallographic Data Centre via "<https://www.ccdc.cam.ac.uk/mystructures/structuredetails/81620710-4b7a-ef11-96c9-00505695281c>" (deposited and accessed on 24 September 2024)". The monocrystals, which generally were difficult to obtain, were in the case of compound **3l** grown from anhydrous ethyl acetate and DCM (3:7) by slow evaporation over approximately ten days after a large screening of gradients of all the usual solvents. Unfortunately, the application of similar conditions to other derivatives reported in this paper, specifically **3d**, **3k**, and **3m**, failed to

obtain their X-ray crystal structure. The solid compounds obtained in all the latter cases were found to be amorphous.

For crystal, structural, and refinement statistics, see the ESI. The important facts are shown in part (a) and (b) of Figure 3. The crystal of the titled molecule **3I** is governed by an intermolecular O₁(of SO₂ group)–H(C₆ of monosubstituted phenyl group) and O₂(of SO₂ group)–H(of C₁₈ of monosubstituted phenyl group) interactions. There are four of these H-bonds (S=O–H–Csp²) in the crystal unit cell, but only two types, which ensures the cohesion of only two molecules of **3I**.

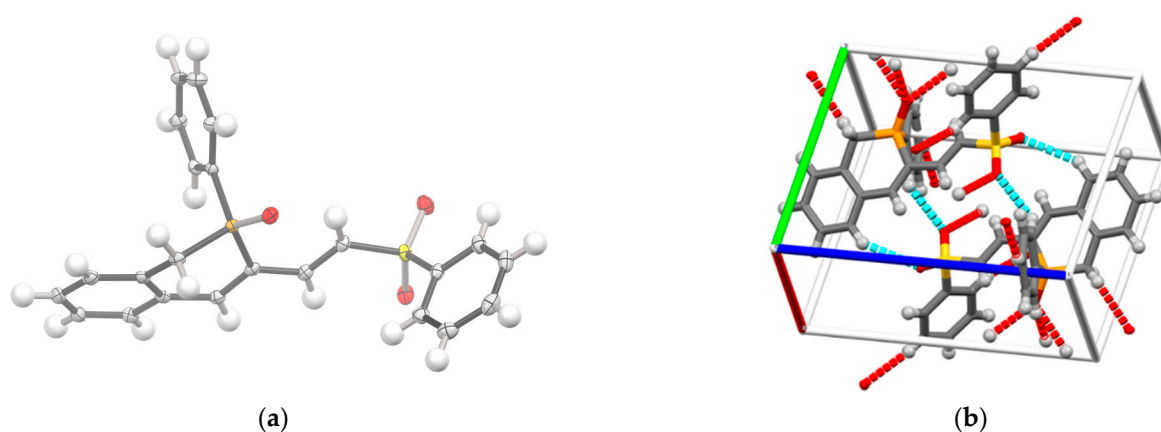


Figure 3. (a) X-ray molecular structure with atom labelling and thermal ellipsoids at 50% level for **3I**. (b) Packing structure in the crystal, together with the crystal unit cell, indicating 4 H-bonds in blue-sky between two molecules of **3I**.

5. Conclusions

These preliminary results represent the first investigation on the regioselective C2-functionalization of a phospho-heterocycle, 2-phenyl-1*H*-isophosphinoline 2-oxide (**1**) with olefins containing different substituents. The coupling products **3a–m** were obtained using a catalytic system comprising both Ag₂CO₃ and palladium(II) acetate, with yields ranging from 21% to 87%. The C-H functionalization occurred selectively at the alpha position of the 2-phenyl-1*H*-isophosphinoline 2-oxide core forming from monosubstituted alkenes exclusively, then *E*-isomers proved by X-ray analysis of product **3I** (CCDC-2386195) as representative example. In a second investigation, the flame-retardant properties of selected molecules were examined. It was clearly demonstrated that the association of a phosphine oxide with another heteroatom-carrying group has positive synergistic effects enabling action in the condensed phase that is not seen in pure phosphine oxide FRs.

6. Material and Methods

6.1. Analytical Data

¹H, ¹³C{¹H}, and ³¹P{¹H} NMR spectra were recorded with a Bruker Avance 400 MHz spectrometer. The chemical shifts were recorded as follows: the chemical shift was measured in parts per million (ppm), and the coupling constants (*J*) were reported in Hz. Multiplicities were reported as singlet (s), broad singlet (bs), doublet (d), triplet (t), quartet (q), quintet (quin), and multiplet (m). High resolution mass spectroscopic (HRMS) analysis was performed on a Xevo G2 Q TOF spectrometer using the electrospray method by the Laboratoire de Mesures Physiques of the University of Montpellier. All reactions were run under an atmosphere of nitrogen using standard Schlenk techniques otherwise stated.

6.2. Thermogravimetric Analysis (TGA)

Thermogravimetric analyses (TGA) were performed using a TGA Q50 (TA instrument) at a heating rate of 20 °C.min⁻¹. Two to eight milligrams of each sample was placed on a platinum pan and heated from room temperature to 800 °C under nitrogen flow

(60 mL.min⁻¹). The temperature at 5% weight loss, the temperature at the maximum rate of weight loss, the rate at the maximum degradation temperature, and the char yield at 750 °C were measured.

6.3. Microscale Combustion Calorimetry (MCC)

A microscale combustion calorimeter (also called a pyrolysis-combustion flow calorimeter or PCFC) from Fire Testing Technologies was used to assess the flammability of some isophosphinolines. The samples (2–5 mg) first underwent an anaerobic pyrolysis step (1 K/s) from 100 to 750 °C under nitrogen flow (100 mL/min). The gases from pyrolysis were sent to a combustor, where they were fully oxidized at 900 °C in the presence of a nitrogen–oxygen mixture (80/20, with oxygen in excess). The heat release rate was calculated according to the well-known Huggett relation (1 g of oxygen consumed corresponds to 13.1 kJ of energy released). The heat release rate was plotted versus the pyrolysis temperature. The residue content was also measured at the end of the test, and the heat of complete combustion (Δh in kJ.g⁻¹) was calculated as the ratio between the total heat release (i.e., the area under the HRR curve versus temperature of pyrolysis) and the residue fraction.

6.4. General Procedures

A Typical Procedure for the Synthesis of C-H Alkenated Products 3a–m

In a sealed tube, the 2-phenyl-1*H*-isophosphinoline oxide (**1**, 0.416 mmol, 1 eq.), a suitable alkene (0.486 mmol, 1.17 eq.) and silver carbonate (0.486 mmol, 1.17 eq.) were dissolved in pivalic acid 4 mL (solid at rt, and heated with a hit gun in order to sample). Pd(OAc)₂ (10 mol%, 0.0486 mmol, 0.117 eq.) was then added, and the reaction mixture was stirred at 90 °C for 20 h. After cooling to rt, the reaction mixture was poured into a saturated solution of K₂CO₃ (20 mL) and left to stir for 20 h. Then, after extraction of the solution with DCM (3 × 15 mL), the collected organic layers were dried over MgSO₄, filtered, and evaporated under reduced pressure. Purification on flash chromatography of the residue was performed to provide the expected compounds **3a–m** in appreciable to good yields.

6.5. Experimental Data

(*E*)-2-Phenyl-3-styryl-1*H*-isophosphinoline 2-oxide (**3a**). ³¹P NMR (162 MHz, CDCl₃) δ 23.09. ¹H NMR (400 MHz, CDCl₃) δ 7.98–7.64 (m, 1H), 7.57–7.06 (m, 9H), 6.90 (ddd, $J = 20.3, 16.4, 0.9$ Hz, 1H), 3.76 (ddd, $J = 22.2, 17.1, 1.1$ Hz, 1H), 3.57–3.19 (m, 1H). ¹³C NMR (101 MHz, CDCl₃) δ 141.89 (d, $J = 6.1$ Hz), 137.14, 134.13 (d, $J = 5.5$ Hz), 132.70 (d, $J = 13.6$ Hz), 132.20 (d, $J = 2.8$ Hz), 130.56 (d, $J = 6.1$ Hz), 130.49 (d, $J = 2.7$ Hz), 130.34 (d, $J = 10.1$ Hz), 128.82 (d, $J = 12.0$ Hz), 128.07 (d, $J = 13.1$ Hz), 127.72 (d, $J = 187.3$ Hz), 126.75, 35.23 (d, $J = 70.6$ Hz). HRMS: m/z calcd for C₂₃H₂₀OP 343.12463 [M + H]⁺, found 343.12466. Yield: 57%; 82 mg; eluent: ethyl acetate/petroleum ether (7:3).

(*Z*)-3-(1,2-Diphenylvinyl)-2-phenyl-1*H*-isophosphinoline 2-oxide (**3b**). ³¹P NMR (162 MHz, CDCl₃) δ 22.68. ¹H NMR (400 MHz, CDCl₃) δ 8.19–6.35 (m, 21H), 3.76 (dd, $J = 21.1, 17.1$ Hz, 1H), 3.44 (dd, $J = 17.2, 12.0$ Hz, 1H). ¹³C NMR (101 MHz, CDCl₃) δ 142.87 (d, $J = 6.5$ Hz), 136.73, 132.95 (d, $J = 5.9$ Hz), 132.04, 130.94, 130.58, 130.48, 130.30, 130.16, 129.90, 129.57, 129.44, 129.36, 129.06, 128.84, 128.72, 128.38, 128.01, 127.84, 127.15, 35.75 (d, $J = 71.0$ Hz). HRMS: m/z calcd for C₂₉H₂₃OP 419.15613 [M + H]⁺, found 419.15601. Yield: 29%; 51 mg; eluent: ethyl acetate/petroleum ether (7:3).

3-(Cyclohex-2-en-1-yl)-2-phenyl-1*H*-isophosphinoline 2-oxide (**3c**). ³¹P NMR (162 MHz, CDCl₃) 2 diastereomers: δ 24.17 (36%), 22.9 (64%). ¹H NMR (400 MHz, CDCl₃) δ 7.69 (m, 10H), 6.09–5.35 (m, 2H), 3.81–3.52 (m, 1H), 3.41–3.20 (m, 1H), 2.15–0.85 (m, 7H). ¹³C NMR (101 MHz, CDCl₃) δ 141.26 (d, $J = 6.7$ Hz), 140.84 (d, $J = 6.8$ Hz), 137.63 (d, $J = 87.2$ Hz), 137.01 (d, $J = 88.0$ Hz), 133.97–132.32 (m), 132.45–127.58 (m), 36.55 (d, $J = 8.0$ Hz), 35.67 (d, $J = 7.4$ Hz), 34.79 (d, $J = 69.6$ Hz), 34.73 (d, $J = 69.5$ Hz), 30.23 (d, $J = 2.2$ Hz), 29.82, 29.25 (d, $J = 2.5$ Hz), 24.99, 20.03, 19.96. HRMS: m/z calcd for C₂₁H₂₂OP 321.14028 [M + H]⁺, found 321.14038. Yield: 38; 51 mg; eluent: ethyl acetate/petroleum ether (9:1).

Dimethyl (*E*)-(2-(2-oxido-2-phenyl-1*H*-isophosphinolin-3-yl)vinyl)phosphonate (**3d**). ³¹P NMR (162 MHz, CDCl₃) δ 21.34 (d, *J* = 3.4 Hz), 21.05 (d, *J* = 3.4 Hz). ¹H NMR (400 MHz, CDCl₃) δ 7.66–7.55 (m, 2H), 7.49–7.09 (m, 10H), 6.27 (td, *J* = 17.7, 1.3 Hz, 1H), 3.75–3.65 (m, 1H), 3.61 (d, *J* = 11.2 Hz, 3H), 3.42 (d, *J* = 11.2 Hz, 3H), 3.35 (dd, *J* = 17.3, 12.4 Hz, 1H). ¹³C NMR (101 MHz, CDCl₃) δ 148.61 (d, *J* = 5.9 Hz), 147.09, 132.50 (d, *J* = 2.9 Hz), 132.39, 131.51 (d, *J* = 13.3 Hz), 130.95, 130.90, 130.82, 130.71, 130.39, 130.29, 128.99, 128.87, 128.60, 128.25, 127.84 (d, *J* = 25.3 Hz), 118.90 (d, *J* = 4.5 Hz), 117.05 (d, *J* = 4.4 Hz). HRMS: *m/z* calcd for C₁₉H₂₁O₄P₂ 375.09096 [M + H]⁺, found 375.09100. Yield: 50%; 78 mg; eluent: ethyl acetate/petroleum ether (97.5:2.5).

Diethyl (*E*)-(2-(2-oxido-2-phenyl-1*H*-isophosphinolin-3-yl)vinyl)phosphonate (**3e**). ³¹P NMR (162 MHz, CDCl₃) δ 21.21 (d, *J* = 3.4 Hz), 18.05 (d, *J* = 3.4 Hz). ¹H NMR (400 MHz, CDCl₃) δ 7.79–7.62 (m, 2H), 7.55–7.09 (m, 9H), 6.53–6.23 (m, 1H), 4.09–3.96 (m, 2H), 3.89–3.66 (m, 3H), 3.40 (m, *J* = 12.3, 0.9 Hz, 1H), 1.29 (td, *J* = 7.1, 0.6 Hz, 3H), 1.10 (td, *J* = 7.0, 0.5 Hz, 3H). ¹³C NMR (101 MHz, CDCl₃) δ 148.27, 146.27 (t, *J* = 6.5 Hz), 132.67, 132.45, 131.74 (d, *J* = 2.3 Hz), 131.56, 130.98, 130.46 (d, *J* = 10.0 Hz), 128.93 (d, *J* = 12.2 Hz), 128.26, 120.66 (d, *J* = 4.5 Hz), 118.82 (d, *J* = 4.4 Hz), 61.92 (dd, *J* = 23.4, 5.3 Hz), 35.23 (d, *J* = 70.7 Hz), 16.28 (s). HRMS: *m/z* calcd for C₂₁H₂₅OP 403.12226 [M + H]⁺, found 403.12234. Yield: 87%; 145 mg; eluent: ethyl acetate/MeOH (95:5).

Methyl (*E*)-3-(2-oxido-2-phenyl-1*H*-isophosphinolin-3-yl)acrylate (**3f**). ³¹P NMR (162 MHz, CDCl₃) δ 21.20. ¹H NMR (400 MHz, CDCl₃) δ 7.78–7.63 (m, 2H), 7.58–7.04 (m, 9H), 6.55 (d, *J* = 16.1 Hz, 1H), 3.76 (d, *J* = 1.2 Hz, 1H), 3.69 (s, 3H), 3.41 (d, *J* = 17.3 Hz, 1H). ¹³C NMR (101 MHz, CDCl₃) δ 167.29, 148.57 (d, *J* = 5.8 Hz), 142.26 (d, *J* = 5.8 Hz), 132.53 (d, *J* = 2.8 Hz), 131.81 (d, *J* = 13.1 Hz), 131.65 (d, *J* = 2.2 Hz), 131.20 (d, *J* = 7.1 Hz), 130.81, 130.80 (d, *J* = 11.2 Hz), 130.28 (d, *J* = 10.1 Hz), 128.99 (d, *J* = 12.2 Hz), 128.42 (d, *J* = 88.9 Hz), 128.27, 51.78, 35.14 (d, *J* = 70.8 Hz). HRMS: *m/z* calcd for C₁₉H₁₈O₃P 325.09881 [M + H]⁺, found 325.09885. Yield: 59%; 81 mg; eluent: ethyl acetate/petroleum ether (9:1).

(*E*)-*N,N*-Dimethyl-3-(2-oxido-2-phenyl-1*H*-isophosphinolin-3-yl)acrylamide (**3g**). ³¹P NMR (162 MHz, CDCl₃) δ 21.94. ¹H NMR (400 MHz, CDCl₃) δ 7.67 (ddd, *J* = 12.2, 8.4, 1.4 Hz, 2H), 7.53–7.20 (m, 8H), 7.15 (d, *J* = 7.3 Hz, 1H), 7.02 (dd, *J* = 15.4, 1.3 Hz, 1H), 3.74 (dd, *J* = 21.9, 17.2 Hz, 1H), 3.40 (dd, *J* = 17.2, 12.6 Hz, 1H), 2.93 (s, 3H), 2.87 (s, 3H). ¹³C NMR (101 MHz, CDCl₃) δ 147.71 (d, *J* = 6.1 Hz), 139.77 (d, *J* = 5.7 Hz), 132.55 (d, *J* = 88.3 Hz), 132.36 (d, *J* = 2.9 Hz), 131.99, 131.42 (d, *J* = 2.6 Hz), 130.62, 128.91 (d, *J* = 12.1 Hz), 128.57 (d, *J* = 11.8 Hz), 128.19, 122.72 (d, *J* = 4.1 Hz), 36.58 (d, *J* = 144.0 Hz), 35.17 (d, *J* = 70.6 Hz). HRMS: *m/z* calcd for C₂₀H₂₁O₂NP 338.13044 [M + H]⁺, found 338.13052. Yield: 25%; 35 mg; eluent: ethyl acetate/MeOH (95:5).

(*E*)-3-(2-Oxido-2-phenyl-1*H*-isophosphinolin-3-yl)acrylonitrile (**3h**). ³¹P NMR (162 MHz, CDCl₃) δ 21.75. ¹H NMR (400 MHz, CDCl₃) δ 7.69–7.49 (m, 3H), 7.47–7.30 (m, 6H), 7.23–7.01 (m, 2H), 6.24 (d, *J* = 16.9 Hz, 1H), 3.82 (ddd, *J* = 23.0, 17.3, 1.0 Hz, 1H), 3.43 (dd, *J* = 17.3, 13.1 Hz, 1H). ¹³C NMR (101 MHz, CDCl₃) δ 148.93 (d, *J* = 5.3 Hz), 148.09 (d, *J* = 5.8 Hz), 132.87 (d, *J* = 2.9 Hz), 132.02 (d, *J* = 2.3 Hz), 131.59 (d, *J* = 64.3 Hz), 131.37, 131.11 (d, *J* = 6.9 Hz), 130.89 (d, *J* = 11.5 Hz), 130.02 (d, *J* = 10.1 Hz), 129.12 (d, *J* = 12.3 Hz), 128.47, 128.06, 127.19, 118.00, 101.65 (d, *J* = 4.9 Hz), 34.80 (d, *J* = 71.1 Hz). HRMS: *m/z* calcd for C₁₈H₁₅ONP 292.08858 [M + H]⁺, found 292.08859. Yield: 44%; 54 mg; eluent: DCM/MeOH (95:5).

Methyl 2-methyl-3-(2-oxido-2-phenyl-1*H*-isophosphinolin-3-yl)acrylate (**3ia**). ³¹P NMR (162 MHz, CDCl₃) δ 21.29 (s). ¹H NMR (400 MHz, CDCl₃) δ 7.70–7.65 (m, 2H), 7.50 (d, *J* = 7.5 Hz, 1H), 7.41 (t, *J* = 7.4 Hz, 2H), 7.36–7.26 (m, 5H), 7.20 (d, *J* = 7.0 Hz, 1H), 3.79 (d, *J* = 17.3 Hz, 1H), 3.70 (s, 3H), 3.44–3.39 (m, 1H), 2.05 (d, *J* = 1.5 Hz, 3H). ¹³C NMR (101 MHz, CDCl₃) δ 184.02 (s), 168.16 (s), 145.12 (d, *J* = 5.1 Hz), 133.59 (d, *J* = 6.9 Hz), 132.51 (d, *J* = 2.8 Hz), 131.73 (dd, *J* = 12.0, 6.2 Hz), 131.13 (d, *J* = 2.5 Hz), 131.00 (d, *J* = 10.9 Hz), 130.63 (d, *J* = 9.9 Hz), 130.58 (s), 130.21 (s), 129.44 (d, *J* = 7.0 Hz), 128.90 (d, *J* = 12.2 Hz), 128.16 (s), 52.19 (s), 36.44–32.84 (m), 14.88 (s). HRMS: *m/z* calcd for C₂₀H₁₉O₃P 339,1145 [M + H]⁺, found 339,1144. Yield: 4%; 63 mg; eluent: ethyl acetate/MeOH (97.5:2.5).

Methyl 2-((2-oxido-2-phenyl-1*H*-isophosphinolin-3-yl)methyl)acrylate (**3ib**). ^{31}P NMR (162 MHz, CDCl_3) δ 23.13. ^1H NMR (400 MHz, CDCl_3) δ 7.64 (ddd, $J = 11.9, 8.3, 1.4$ Hz, 2H), δ 7.53–7.34 (m, 3H), 7.31–7.17 (m, 4H), 7.15–6.92 (m, 2H), 6.23 (d, $J = 1.2$ Hz, 1H), 5.68 (d, $J = 1.3$ Hz, 1H), 3.60 (s, 3H), 3.40 (d, $J = 10.6$ Hz, 2H), 3.33 (dd, $J = 17.2, 12.5$ Hz, 1H). ^{13}C NMR (101 MHz, CDCl_3) δ 142.19 (d, $J = 6.4$ Hz), 132.24 (d, $J = 2.9$ Hz), 130.81, 130.71, 130.62, 130.29, 129.61, 129.36, 128.72 (d, $J = 12.0$ Hz), 127.95, 51.97, 34.40 (d, $J = 70.1$ Hz), 33.50 (d, $J = 8.2$ Hz). HRMS: m/z calcd for $\text{C}_{20}\text{H}_{20}\text{O}_3\text{P}$ 339.11446 $[\text{M} + \text{H}]^+$, found 339.11450. Yield: 10%; 143 mg; eluent: ethyl acetate/MeOH (97.5:2.5).

Methyl 3-(2-oxido-2-phenyl-1*H*-isophosphinolin-3-yl)-2-((2-oxido-2-phenyl-1*H*-isophosphinolin-3-yl)methyl)acrylate (**3ic**). ^{31}P NMR (162 MHz, Chloroform-*d*) δ 22.84 (d, $J = 24.9$ Hz), 21.86 (d, $J = 18.3$ Hz). ^1H NMR (400 MHz, CDCl_3) δ 7.80–7.52 (m, 5H), 7.52–7.30 (m, 6H), 7.30–7.08 (m, 7H), 6.86 (dd, $J = 72.0, 33.0$ Hz, 1H), 3.76–3.63 (m, 3H), 3.64–3.54 (m, 2H), 3.55–3.22 (m, 3H), 1.24 (t, $J = 7.1$ Hz, 3H). ^{13}C NMR (101 MHz, CDCl_3) δ 167.14 (d, $J = 10.1$ Hz), 144.80 (dd, $J = 42.8, 4.2$ Hz), 140.41 (dd, $J = 12.0, 6.1$ Hz), 136.47 (dd, $J = 24.4, 7.7$ Hz), 132.60–132.21 (m), 132.22–131.96 (m), 132.27–131.41 (m), 131.11 (dd, $J = 12.9, 6.6$ Hz), 131.01–130.24 (m), 130.40–129.64 (m), 129.53 (s), 129.23–128.59 (m), 128.36 (s), 128.23 (d, $J = 11.4$ Hz), 127.89 (d, $J = 10.7$ Hz), 127.21 (d, $J = 52.4$ Hz), 60.43 (s), 52.19 (d, $J = 1.9$ Hz), 35.21–33.21 (m), 29.87–28.84 (m). HRMS: m/z calcd for $\text{C}_{35}\text{H}_{30}\text{O}_4\text{P}_2$ 577.1692 $[\text{M} + \text{H}]^+$, found 577.1692. Yield: 25%; 343 mg; eluent: ethyl acetate/MeOH (97.5:2.5).

Ethyl 2-((2-oxido-2-phenyl-1*H*-isophosphinolin-3-yl)methyl)acrylate (**3ja**). ^{31}P NMR (162 MHz, CDCl_3) δ 21.11 (s). ^1H NMR (400 MHz, CDCl_3) δ 7.73–7.64 (m, 2H), 7.52 (ddt, $J = 6.7, 4.2, 1.4$ Hz, 1H), 7.47–7.39 (m, 2H), 7.37–7.26 (m, 5H), 7.21 (d, $J = 6.9$ Hz, 1H), 4.22–4.06 (m, 2H), 3.72 (dd, $J = 20.8, 17.2$ Hz, 1H), 3.40 (dd, $J = 17.2, 11.7$ Hz, 1H), 2.06 (t, $J = 1.6$ Hz, 3H), 1.24 (t, $J = 7.1$ Hz, 3H). ^{13}C NMR (101 MHz, CDCl_3) δ 167.86 (s), 145.01 (d, $J = 4.9$ Hz), 133.62 (d, $J = 6.9$ Hz), 132.56 (d, $J = 2.7$ Hz), 132.37–131.82 (m), 131.16 (d, $J = 12.5$ Hz), 130.85 (d, $J = 9.8$ Hz), 130.66 (s), 130.28 (s), 130.14 (s), 129.25 (s), 129.02 (d, $J = 12.1$ Hz), 128.29 (s), 61.22 (s), 34.89 (d, $J = 70.1$ Hz), 14.75 (d, $J = 56.1$ Hz). HRMS: m/z calcd for $\text{C}_{21}\text{H}_{22}\text{O}_3\text{P}$ 353.13011 $[\text{M} + \text{H}]^+$, found 353.13019. Yield: 4%; 12 mg; eluent: ethyl acetate/MeOH (97.5:2.5).

Ethyl 2-((2-oxido-2-phenyl-1*H*-isophosphinolin-3-yl)methyl)acrylate (**3jb**). ^{31}P NMR (162 MHz, Chloroform-*d*) δ 23.10. ^1H NMR (400 MHz, Chloroform-*d*) δ 7.65 (ddd, $J = 11.9, 8.3, 1.4$ Hz, 2H), 7.47 (m, 1H), 7.43–7.34 (m, 2H), 7.31–7.16 (m, 3H), 7.15–6.99 (m, 2H), 6.23 (d, $J = 1.3$ Hz, 1H), 5.68 (d, $J = 1.2$ Hz, 1H), 4.08 (m, 2H), 3.67 (dd, $J = 21.7, 17.1$ Hz, 1H), 3.41 (d, $J = 10.6$ Hz, 2H), 3.33 (dd, $J = 17.1, 12.4$ Hz, 1H), 1.19 (t, $J = 7.1$ Hz, 3H). ^{13}C NMR (101 MHz, Chloroform-*d*) δ 142.00 (d, $J = 6.3$ Hz), 132.42 (d, $J = 14.8$ Hz), 132.16, 131.55, 130.80, 130.71, 130.67 (d, $J = 72.1$ Hz), 130.62, 130.21, 129.07, 129.01, 128.76, 128.64, 127.93, 60.87, 35.24–33.11 (m), 14.27. HRMS: m/z calcd for $\text{C}_{21}\text{H}_{22}\text{O}_3\text{P}$ 353.13011 $[\text{M} + \text{H}]^+$, found 353.13019. Yield: 31%; 91 mg; eluent: ethyl acetate/MeOH (97.5:2.5).

Ethyl 3-(2-oxido-2-phenyl-1*H*-isophosphinolin-3-yl)-2-((2-oxido-2-phenyl-1*H*-isophosphinolin-3-yl)methyl)acrylate (**3jc**). ^{31}P NMR (162 MHz, CDCl_3) δ 22.69 (d, $J = 25.4$ Hz), 21.70 (d, $J = 8.4$ Hz). ^1H NMR (400 MHz, CDCl_3) δ 7.80–7.58 (m, 4H), 7.58–7.46 (m, 2H), 7.46–7.27 (m, 7H), 7.26–7.10 (m, 4H), 6.87 (dd, $J = 63.3, 33.0$ Hz, 1H), 4.12 (dd, $J = 14.4, 7.2$ Hz, 2H), 4.08–4.01 (m, 1H), 3.67 (ddd, $J = 21.2, 17.8, 8.3$ Hz, 3H), 3.55–3.29 (m, 2H), 1.28–1.22 (m, 3H), 1.16 (dt, $J = 9.1, 7.1$ Hz, 3H). ^{13}C NMR (101 MHz, CDCl_3) δ 166.71 (d, $J = 9.9$ Hz), 144.84 (t, $J = 19.1$ Hz), 144.52 (d, $J = 4.2$ Hz), 140.80–139.93 (m), 136.21 (dd, $J = 26.1, 7.7$ Hz), 132.28 (d, $J = 5.6$ Hz), 132.11 (d, $J = 3.3$ Hz), 132.05 (s), 131.08–130.07 (m), 129.83 (dt, $J = 14.5, 7.2$ Hz), 129.27–128.59 (m), 128.24 (d, $J = 11.9$ Hz), 128.02 (d, $J = 3.9$ Hz), 127.89 (d, $J = 10.2$ Hz), 127.41 (d, $J = 53.6$ Hz), 61.12 (d, $J = 4.2$ Hz), 60.41 (s), 35.30–33.62 (m), 29.91–29.01 (m), 21.08 (s), 15.11–13.39 (m). HRMS: m/z calcd for $\text{C}_{36}\text{H}_{33}\text{O}_4\text{P}_2$ 591.1849.13011 $[\text{M} + \text{H}]^+$, found 591.1847. Yield: 27%; 78 mg; eluent: ethyl acetate/MeOH (97.5:2.5).

(*E*)-*N*-(4-Methoxybenzyl)-3-(2-oxido-2-phenyl-1*H*-isophosphinolin-3-yl)acrylamide (**3k**). ^{31}P NMR (162 MHz, CDCl_3) δ 23.57. ^1H NMR (400 MHz, CDCl_3) δ 7.59 (dd, $J = 12.3, 7.6$ Hz, 2H), 7.47 (td, $J = 15.4, 14.9, 10.2$ Hz, 3H), 7.34 (m, 5H), 7.16 (d, $J = 8.2$ Hz, 2H), 7.11 (d, $J = 7.5$ Hz, 1H), 6.80 (d, $J = 8.2$ Hz, 2H), 6.73 (d, $J = 15.5$ Hz, 1H), 6.29 (s, 1H), 4.45 (dd,

$J = 14.7, 5.8$ Hz, 1H), 4.35 (dd, $J = 14.6, 5.4$ Hz, 1H), 3.75 (s, 3H), 3.71–3.58 (m, 1H), 3.30 (dd, $J = 17.2, 13.5$ Hz, 1H). ^{13}C NMR (101 MHz, CDCl_3) δ 165.6, 159.0, 147.8–147.7 (d), 138.7 (d), 132.5 (d), 132.1–132 (d), 131.40 (d), 131.0–130.9 (d), 130.6, 130.5, 130.40, 130.2–130.1 (d), 129.4, 129.0–128.8 (d), 128.2, 125.9, 114.1, 55.33, 43.37, 29.83. HRMS (APPI+): Calculated for $\text{C}_{26}\text{H}_{24}\text{NO}_3\text{P}$ $[\text{M}+\text{H}]^+$ 430.1566 found 430.1561. Yield 31%, 28 mg; eluent: ethyl acetate/dichloromethane (1:1).

(*E*)-2-Phenyl-3-(2-(phenylsulfonyl)vinyl)-1*H*-isophosphinoline 2-oxide (**3l**). ^{31}P NMR (162 MHz, CDCl_3) δ 21.77. ^1H NMR (400 MHz, CDCl_3) δ 7.80 (d, $J = 7.7$ Hz, 2H), 7.56 (dd, $J = 11.2, 5.8$ Hz, 4H), 7.46 (q, $J = 6.5, 5.0$ Hz, 5H), 7.35 (qd, $J = 11.0, 10.0, 7.4$ Hz, 5H), 7.16 (m, 2H), 3.76 (dd, $J = 22.5, 17.2$ Hz, 1H), 3.41 (dd, $J = 17.3, 12.9$ Hz, 1H). ^{13}C NMR (101 MHz, CDCl_3) δ 150.5–150.4 (d), 140.5, 139.8–139.7 (d), 133.4, 132.8–132.7 (d), 132.0 (d), 131.8, 131.5, 131.4, 131.3 (d), 131.0–130.8 (d), 130.1–130.0 (d), 129.3, 129.1–129.0 (d), 128.4, 128.0, 127.0, 126.1, 35.1–34.4 (d). HRMS (APPI+): Calculated for $\text{C}_{23}\text{H}_{19}\text{O}_3\text{PS}$ $[\text{M}+\text{H}]^+$ 407.0865 found 407.0862. Yield 37%, 31 mg; eluent: ethyl acetate/DCM (3:7).

(*E*)-2-(2-(2-Oxido-2-phenyl-1*H*-isophosphinolin-3-yl)vinyl)isoindoline-1,3-dione (**3m**). ^{31}P NMR (162 MHz, CDCl_3) δ 22.33. ^1H NMR (400 MHz, CDCl_3) δ 7.83 (dt, $J = 7.3, 3.7$ Hz, 2H), 7.77–7.70 (m, 5H), 7.62 (d, $J = 15.2$ Hz, 1H), 7.53–7.46 (m, 2H), 7.41 (td, $J = 7.6, 2.9$ Hz, 2H), 7.30 (d, $J = 4.0$ Hz, 2H), 7.23 (d, $J = 3.2$ Hz, 1H), 7.16 (d, $J = 7.5$ Hz, 1H), 3.79 (dd, $J = 22.5, 17.1$ Hz, 1H), 3.43 (dd, $J = 17.2, 12.8$ Hz, 1H). ^{13}C NMR (101 MHz, CDCl_3) δ 168.1, 146.2, 142.0–141.90 (d), 134.7, 134.4, 133.0, 132.7–132.6 (d), 132.3 (d), 132.0, 131.8, 130.6 (d), 130.5–130.4 (d), 130.3 (d), 129.6, 129.3, 129.0–128.8 (d), 128.1, 123.8, 123.7, 122.2 (d), 118.5 (d), 35.4–34.7 (d). HRMS (APPI+): Calculated for $\text{C}_{25}\text{H}_{18}\text{NO}_3\text{P}$ $[\text{M}+\text{H}]^+$ 412.1097 found 412.1091. Yield 21%, 20 mg, eluent: ethyl acetate/DCM (2:8).

Supplementary Materials: The following supporting information can be downloaded at: <https://www.mdpi.com/article/10.3390/molecules29215104/s1>, Figures S1–S17: $^{31}\text{P}\{^1\text{H}\}$, ^1H and $^{13}\text{C}\{^1\text{H}\}$ NMR and HRMS spectra of the synthesized compounds.

Author Contributions: The individual contributions of all co-authors of this paper are as follows. D.V., T.A. and J.-L.P. first conceived the project and study. K.-P.M.M.N., M.H., C.S., K.A. and A.R.I.I. performed the synthesis and the NMR experiments. G.M.-M., J.L., I.A.T. and F.D. for the supervision of PhD students during their stay in France and abroad. C.N., R.S. and L.D. have explored different kinds of the flame-retardant properties of the synthesized compounds. Finally, T.A. and J.-L.P. wrote collectively the manuscript and G.M.-M., A.D., D.V., T.A. and J.-L.P. provided for their part guidance throughout the project and participated to the supervision the study. All authors have read and agreed to the published version of the manuscript.

Funding: We thank warmly the Normand region, the Normand Institute ‘INC3M FR-CNRS 3038’, Le Havre Seine Métropole (LHSM), and the University of Le Havre Normandie for their financial support and the Scholarship attributed to Christine Safi and Kouceila Abdelli. We thank also the French Embassy in Niger for the financial support and the Scholarship attributed to one of us, Abdou Rachid Issaka Ibrahim. The Ministry of Science, Research and Technology of the Islamic Republic of Iran is gratefully acknowledged for the financial support provided to M.H. (Ph.D. student at the K. N. Toosi University of Technology of Tehran, Iran). The crystal structure determination was performed with the support of our colleague, Sergiu Shova, from Petru Poni’ Institute of Macromolecular Chemistry of Iasi, Romania (shova@icmpp.ro).

Institutional Review Board Statement: Not applicable.

Informed Consent Statement: Not applicable.

Data Availability Statement: Data contained within the article or Supplementary Materials.

Conflicts of Interest: The authors declare no conflicts of interest.

References

1. Campeau, L.-C.; Hazar, N. Cross-Coupling and Related Reactions: Connecting Past Success to the Development of New Reactions for the Future. *Organometallics* **2019**, *38*, 3–35. [[CrossRef](#)] [[PubMed](#)]

2. Chen, Z.; Wang, B.; Zhang, J.; Yu, W.; Liu, Z.; Zhang, Y. Transition metal-catalyzed C–H bond functionalizations by the use of diverse directing groups. *Org. Chem. Front.* **2015**, *2*, 1107–1295. [[CrossRef](#)]
3. Gandeepan, P.; Müller, T.; Zell, D.; Cera, G.; Warratz, S.; Ackermann, L. 3d Transition Metals for C–H Activation. *Chem. Rev.* **2019**, *119*, 2192–2452. [[CrossRef](#)] [[PubMed](#)]
4. Docherty, J.H.; Lister, T.M.; McArthur, G.; Findlay, M.T.; Domingo-Legarda, P.; Kenyon, J.; Choudhary, S.; Larrosa, I. Transition-Metal-Catalyzed C–H Bond Activation for the Formation of C–C Bonds in Complex Molecules. *Chem. Rev.* **2023**, *123*, 7692–7760. [[CrossRef](#)]
5. Wang, Y.F.; Wang, C.J.; Feng, Q.Z.; Zhai, J.J.; Qi, S.S.; Zhong, A.G.; Chu, M.M.; Xu, D.Q. Copper-catalyzed asymmetric 1,6-conjugate addition of in situ generated para-quinone methides with b-ketoesters. *Chem. Commun.* **2022**, *58*, 6653–6656. [[CrossRef](#)]
6. Danton, F.; Najjar, R.; Othman, M.; Martin Lawson, A.; Moncol, J.; Ghinet, A.; Rigo, B.; Oulyadi, H.; Daïch, A. Site-Selective Pd-Catalysed Fujiwara-Moritani type Reaction of *N,S*-Heterocyclic Systems with Olefins. *Adv. Synth. Catal.* **2020**, *362*, 1088–1095. [[CrossRef](#)]
7. Liu, S.Y.; Liu, H.; Shen, Z.Q.; Huang, W.Y.; Zhong, A.G.; Wen, H.R. Atom- and step-economic synthesis of π -conjugated large oligomers via CeH activated oligomerization. *Dye. Pigment.* **2019**, *162*, 640–646. [[CrossRef](#)]
8. Wang, L.H.; Chen, X.J.; Ye, D.N.; Liu, H.; Chen, Y.; Zhong, A.G.; Li, C.Z.; Liu, S.Y. Pot- and atom-economic synthesis of oligomeric non-fullerene acceptors via C–H direct arylation. *Polym. Chem.* **2022**, *13*, 2351–2361. [[CrossRef](#)]
9. Bhargav, D.; Monak, P.; Bharatkumar, Z.D.; Sujoy, R.; Togati, N. Recent advances in directed sp^2 C–H functionalization towards the synthesis of *N*-heterocycles and *O*-heterocycles. *Chem. Commun.* **2021**, *57*, 8699–8725. [[CrossRef](#)]
10. Methot, J.L.; Roush, W.R. Nucleophilic Phosphine Organocatalysis. *Adv. Synth. Catal.* **2004**, *346*, 1035–1050. [[CrossRef](#)]
11. Guo, H.; Fan, Y.C.; Sun, Z.; Wu, Y.; Kwon, O. Phosphine Organocatalysis. *Chem. Rev.* **2018**, *118*, 10049–10293. [[CrossRef](#)]
12. Xuan, C.; Zhu, Z.; Li, Z.; Shu, C. Recent Developments in the Synthesis of Pharmacological Alkyl Phosphonates. *Adv. Agrochem.* **2024**; *in press*. [[CrossRef](#)]
13. Virieux, D.; Volle, J.-N.; Bakalara, N.; Pirat, J.-L. Synthesis and Biological Applications of Phosphinates and Derivatives. *Top. Curr. Chem.* **2014**, *360*, 39–114. [[CrossRef](#)]
14. Yu, H.; Yang, H.; Shi, E.; Tang, W. Development and Clinical Application of Phosphorus-Containing Drugs. *Med. Drug Discov.* **2020**, *8*, 100063. [[CrossRef](#)] [[PubMed](#)]
15. Johnson, W.; Bergfeld, W.F.; Belsito, D.V.; Hill, R.A.; Klaassen, C.D.; Liebler, D.C.; Marks, J.G.; Shank, R.C.; Slaga, T.J.; Snyder, P.W.; et al. Safety Assessment of Lecithin and Other Phosphoglycerides as Used in Cosmetics. *Int. J. Toxicol.* **2020**, *39*, 5S–25S. [[CrossRef](#)]
16. Ghorai, A.; Banerjee, S. Phosphorus-Containing Aromatic Polymers: Synthesis, Structure, Properties and Membrane-Based Applications. *Prog. Polym. Sci.* **2023**, *138*, 101646. [[CrossRef](#)]
17. Kloda, M.; Ondrušová, S.; Lang, K.; Demel, J. Phosphinic Acids as Building Units in Materials Chemistry. *Coord. Chem. Rev.* **2021**, *433*, 213748. [[CrossRef](#)]
18. Han, S.-D.; Hu, J.-X.; Li, J.-H.; Wang, G.-M. Anchoring Polydentate *N/O*-Ligands in Metal Phosphite/Phosphate/Phosphonate (MPO) for Functional Hybrid Materials. *Coord. Chem. Rev.* **2023**, *475*, 214892. [[CrossRef](#)]
19. Asok, N.; Gaffen, J.R.; Baumgartner, T. Unique Phosphorus-Based Avenues for the Tuning of Functional Materials. *Acc. Chem. Res.* **2023**, *56*, 536–547. [[CrossRef](#)]
20. Müller, S.M.; Schlögl, S.; Wiesner, T.; Haas, M.; Griesser, T. Recent Advances in Type I Photoinitiators for Visible Light Induced Photopolymerization. *ChemPhotoChem* **2022**, *6*, e202200091. [[CrossRef](#)]
21. Yudaev, P.A.; Kolpinskaya, N.A.; Chistyakov, E.M. Organophosphorous Extractants for Metals. *Hydrometallurgy* **2021**, *201*, 105558. [[CrossRef](#)]
22. Levchik, S.V.; Weil, E.D. A Review of Recent Progress in Phosphorus-Based Flame Retardants. *J. Fire Sci.* **2006**, *24*, 345–364. [[CrossRef](#)]
23. Özer, M.S.; Gaan, S. Recent Developments in Phosphorus Based Flame Retardant Coatings for Textiles: Synthesis, Applications and Performance. *Prog. Org. Coat.* **2022**, *171*, 107027. [[CrossRef](#)]
24. Gao, T.Y.; Wang, F.D.; Xu, Y.; Wei, C.X.; Zhu, S.E.; Yang, W.; Lu, H.D. Luteolin-based epoxy resin with exceptional heat resistance, mechanical and flame retardant properties. *Chem. Eng. J.* **2022**, *428*, 131173–131185. [[CrossRef](#)]
25. Ma, C.; Li, J. Synthesis of an organophosphorus flame retardant derived from daidzein and its application in epoxy. *Compos. Part B* **2019**, *178*, 107471–107482. [[CrossRef](#)]
26. Hariri, M.; Darvish, F.; Mengue Me Ndong, K.-P.; Sechet, N.; Chacktas, G.; Boosaliki, H.; Tran Do, M.L.; Mwanje-Maguene, G.; Lebibi, J.; Burilov, A.R.; et al. Gold-Catalyzed Access to Isophosphinoline 2-Oxides. *J. Org. Chem.* **2021**, *86*, 7813–7824. [[CrossRef](#)]
27. Zhang, Q.; Liu, X.-T.; Wu, Y.; Zhang, Q.-W. Ni-Catalyzed Enantioselective Allylic Alkylation of H-Phosphinates. *Org. Lett.* **2021**, *23*, 8683–8687. [[CrossRef](#)]
28. Huggett, C. Estimation of Rate of Heat Release by Means of Oxygen Consumption Measurements. *Fire Mater.* **1980**, *4*, 61–65. [[CrossRef](#)]
29. Sonnier, R.; Otazaghine, B.; Dumazert, L.; Ménard, R.; Viretto, A.; Dumas, L.; Bonnaud, L.; Dubois, P.; Safronava, N.; Walters, R.; et al. Prediction of thermosets flammability using a model based on group contributions. *Polymer* **2017**, *127*, 203–213. [[CrossRef](#)]
30. Ménard, R.; Negrell-Guirao, C.; Sonnier, R.; Ferry, L.; David, G. Synthesis of biobased phosphate flame retardants. *Pure Appl. Chem.* **2014**, *86*, 1637–1650. [[CrossRef](#)]

31. Seibold, S.; Schäfer, A.; Lohstroh, W.; Walter, O.; Döring, M. Phosphorus-containing terephthalaldehyde adducts-Structure determination and their application as flame retardants in epoxy resins. *J. Appl. Polym. Sci.* **2007**, *108*, 264–271. [[CrossRef](#)]
32. Sicher, J. The syn and anti Steric Course in Bimolecular Olefin-Forming Eliminations. *Angew Chem. Int. Ed. Engl.* **1972**, *11*, 200–214. [[CrossRef](#)]
33. *Rigaku Oxford Diffraction*; CrysAlis Pro Software System; Rigaku Corporation: Oxford, UK, 2015.
34. Sheldrick, G.M. SHELXT—Integrated Space-Group and Crystal-Structure Determination. *Acta Crystallogr. Sect. A Found. Crystallogr.* **2015**, *71*, 3–8. [[CrossRef](#)] [[PubMed](#)]
35. Sheldrick, G.M. Crystal Structure Refinement with SHELXL. *Acta Crystallogr. Sect. C* **2015**, *71*, 3–8. [[CrossRef](#)]
36. Dolomanov, O.V.; Bourhis, L.J.; Gildea, R.J.; Howard, J.A.K.; Puschmann, H. OLEX2: A Complete Structure Solution, Refinement and Analysis Program. *J. Appl. Crystallogr.* **2009**, *42*, 339–341. [[CrossRef](#)]

Disclaimer/Publisher’s Note: The statements, opinions and data contained in all publications are solely those of the individual author(s) and contributor(s) and not of MDPI and/or the editor(s). MDPI and/or the editor(s) disclaim responsibility for any injury to people or property resulting from any ideas, methods, instructions or products referred to in the content.